



Trends and projections of climate extremes in the Black Volta River Basin in West Africa

Fati Aziz¹ · Emmanuel Obuobie² · Mouhamadou Bamba Sylla³ · Jaehak Jeong⁴ · Prasad Daggupati⁵

Received: 14 July 2016 / Accepted: 23 August 2018 / Published online: 5 September 2018
© Springer-Verlag GmbH Austria, part of Springer Nature 2018

Abstract

This study used the RClimDex software to examine trends in extreme air temperature and rainfall in the Black Volta River Basin (BVRB) for the present (1981–2010) and future 2051–2080 (late twenty-first century) horizons. The analysis of the future extreme events was conducted using data output of four ensemble models for two IPCC emission scenarios, Representative Concentration Pathways (RCPs) 4.5 and 8.5. A bias correction method, the quantile-quantile (Q-Q) transformation technique, was applied to all the modelled temperature and rainfall data set prior to the index calculation. The results of analysis of the present-day climate indicate warming and wetting of the BVRB. Increasing trends were seen in the extreme warm indices while the extreme cold indices showed mostly decreasing trends. Majority of the trends observed in the indices were statistically significant (95% confidence level). The extremes in rainfall also showed increasing trends in amounts and intensity of rainfall events (majority of increasing trends were statistically insignificant). Projected temperatures for the late twenty-first century showed decreasing and increasing trends in the cold and warm indices respectively, suggesting warming during the period. Trend analysis of future rainfall projections mostly showed a mix of positive and negative trends offering no clear indication of the direction of change in majority of the extreme rainfall indices. An increase in extremely wet day events is however projected for the period. The results from this study could inform climate change adaptation strategies targeted at reducing vulnerability and building resilience to extreme weather events in the BVRB.

1 Introduction

The latest report of the Intergovernmental Panel on Climate Change (Hartmann et al. 2013: Chapter 2, page 161) highlights that in the last three decades, unprecedented warming

has been recorded at the Earth's surface and temperature will continue to increase as a result of greenhouse gases (GHG) forcing. Under the medium- and high-emissions scenarios, average temperature for large areas of Africa are projected to exceed the 2 °C international threshold by 2050 and reach up to 2.6–4.8 °C by the end of the twenty-first century (CDKN 2014: Chapter 2 page 16). Although Africa's contribution to the overall greenhouse gas emissions has been relatively small, compared to the global emissions, the impacts on water resources, agriculture and ecosystems is expected to be huge due to the low adaptive capacity (Boko et al. 2007).

The IPCC in its Fourth Assessment Report (Solomon et al. 2007) stated that climate change has begun affecting the frequency, intensity and duration of extreme events, some of which are projected to continue. Extreme weather or climate event, popularly termed extreme event, is one of the key manifestations of climate change in a region or an area, and occurs when the “value of a weather or climate variable exceed (or go below) a threshold value near the upper (or lower) ends (‘tails’) of the range of observed values of the variable” (IPCC 2012: Chapter 1, page 30).

✉ Fati Aziz
fatiiaziz17@gmail.com

¹ Laboratoire d'Hydrologie Appliquée, Université D'Abomey-Calavi, Abomey-Calavi, Benin

² Water Research Institute, Council for Scientific and Industrial Research (CSIR), Accra, Ghana

³ West African Science Service Center on Climate Change and Adapted Land use (WASCAL), WASCAL Competence Center, Ouagadougou, Burkina Faso

⁴ Blackland Research and Extension Center, Texas A & M AgriLife Research, Temple, TX, USA

⁵ School of Engineering, University of Guelph, Guelph, Ontario, Canada

Studies conducted on a global scale demonstrate a significant warming in temperature indices during the twentieth century while extreme precipitation trends show a significant wetting trend (Frich et al. 2002; Alexander et al. 2006). Extreme temperature studies conducted in Southern and Western Africa revealed consistent warming during the 1961–2000 period (New et al. 2006). In another study, Mouhamed et al. (2013) also identified a general warming trend over a large area of West Africa for the period 1960–2010. Their study indicated that extreme rainfall events have become more frequent in the West African Sahel during the last decade in comparison to the 1961–1990 period. A study by Gbode et al. (2015) in Kano, Nigeria, revealed increases in the number of cool nights, warm days and in the number of warm spells for the period 1960–2007. Slight increases were also seen in annual total rainfall while the number of extremely wet days increased significantly.

Like several other regions in Africa, the Black Volta River Basin (BVRB), the biggest sub-basin of the Volta River Basin has had to contend with loss of lives, severe damage and large economic and societal losses resulting from unexpected weather conditions. Based on the Köppen-Geiger climate classification, the Black Volta Basin has a largely tropical wet or savannah climate in the south and a smaller hot semi-arid climate in the extreme north (Peel et al. 2007). The basin is shared by Burkina Faso, Ghana, Côte d'Ivoire and Mali. Quite recently in 2007, a massive rainfall caused severe flooding in the region and affected about 54,800 people in Ghana, Burkina Faso and Togo (Tschakert et al. 2010). A flooding episode that hit Burkina Faso, north of the Volta Basin, in 2009 also resulted in serious damages to properties (Ta et al. 2016). Although the basin supports significant economic activities such as fishing, agriculture and energy production, little is known about the trends in extreme precipitation and temperature in the region. Extreme events such as drought and flood episodes over the BVRB can trigger damaging consequences by affecting food security and impacting human wellbeing significantly (Barry et al. 2005). For these reasons, it is necessary to understand the current trends and future projections of changes in temperature and precipitation extremes over the basin to help in exploring the opportunities for managing the risks of weather- and climate-related disasters in the region.

The goal of this study, therefore, was to (1) investigate trends in extreme temperature and precipitation events in the present-day (1981–2010) and late twenty-first century (2051–2080) climate of the Black Volta River Basin and (2) to analyse changes in the trends between the present-day climate and that of the twenty-first century.

2 Data and methodology

2.1 Data

Daily rainfall and minimum and maximum temperature data covering the present horizon (1981–2010) for the 10 synoptic climate stations used in the analysis (Fig. 1) were obtained from the Meteorological Agencies in Ghana and Burkina Faso for the analysis. Only the data of 10 synoptic stations were used because they offered the most reliable data with few gaps during the time of the study. The 10 stations are well distributed across the basin except for the extreme north where there was no observational data available to this study. A higher density of observed station network would have been ideal but considering that the 10 stations used are located in the two climate zones (tropical wet and semi-arid) of the basin, we do not expect any significant changes to the trends in the climate of the basin. We considered similar data for the late twenty-first century (2051–2080) for the IPCC medium-low (RCP4.5) and high (RCP8.5) emission scenarios. The future horizon data obtained from the Coordinated Regional Downscaling experiment (CORDEX) archives were generated from the combination of three RCMs driven by three GCMs (Table 1) for a total of four RCM/GCM scenario combinations. The CORDEX data consists of an ensemble of high-resolution historical and future climate projections at regional scales (Giorgi et al. 2009; Jones et al. 2011) produced by downscaling different Global Climate Models (GCMs) participating in the Coupled Model Intercomparison Project Phase 5 (CMIP5) (Taylor et al. 2012) in combination with RCPs (Moss et al. 2010). Specifically, each climate model output from the CORDEX project is made up of an ensemble of RCM runs, each one of them based on the output of one CMIP5 multi-model ensemble (Taylor et al. 2012), plus evaluation runs driven by ERA-Interim reanalysis data. In effect, the inputs from the CORDEX experiment are very useful for impact and adaptation studies (Giorgi et al. 2009; Jones et al. 2011). Another advantage of the CORDEX data is its high resolution compared with others such as the CMIP5. Whereas the resolution of the CMIP5 GCMs is at best $0.75 \times 0.75^\circ$ and at worst $2.81 \times 2.81^\circ$, for example, that of the CORDEX is approximately $0.44^\circ \times 0.44^\circ$ allowing for more detailed climate change information at regional or local levels (Sylla et al. 2016). The CORDEX RCMs have been validated over Africa (e.g., Nikulin et al. 2012; Panitz et al. 2014; Kim et al. 2014 and Dosio et al. 2015) and in West Africa (e.g., Klutse et al. 2014; Abiodun et al. 2013 and Endris et al. 2015). For more details about the CORDEX RCMs and their experimental set-up, refer to Jones et al. (2011).

The simulations used in this research were downscaled and the raw temperature and precipitation data bias corrected using the quantile-quantile (Q-Q) transformation method (Maraun et al. 2010; Themeßl et al. 2011a, b) to obtain

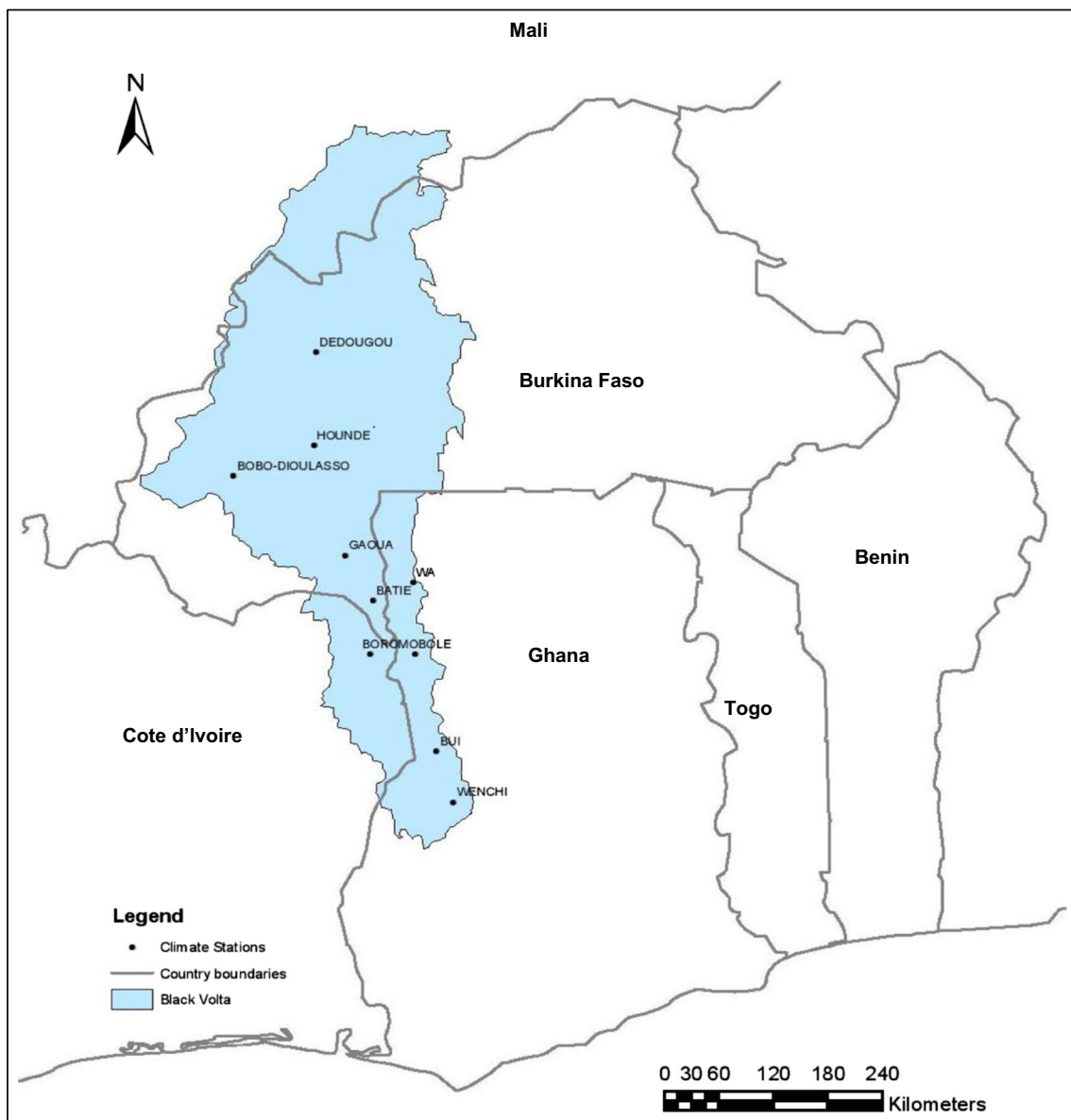


Fig. 1 Map of Black Volta Basin with Meteorological stations used in the study

station-specific future climate scenario data with reduced RCM biases for the extreme index analysis. This was done using a quantile mapping approach that closely follows the methodology in Amadou et al. (2015) and Sarr et al. (2015). The Q-Q transformation technique has been used in several studies to demonstrate its ability in reducing systemic biases. It uses a calibration and validation step; hence, its suitability for the data can be checked by looking the calibration performance using a Kolmogorov-Smirnov test. Results show that the Q-Q transformation always improve similarity between the RCM outputs and the observations on the validation data set (see for instance Sarr et al. 2015). A typical example is the study by Themeßl et al. (2011a, b) over the Alpine region. The study which focused on the application of an ensemble of seven empirical-statistical downscaling and error correction

methods to post-process daily precipitation sums of a high-resolution regional climate hindcast simulation suggested the quantile mapping to be the best in terms of performance, particularly at high quantiles. In their study, improvements were seen in precipitation sums regardless of season and region, indicating the potential transferability of the methods to other regions (Themeßl et al. 2011a, b).

2.2 Methodology

2.2.1 Bias correction in RCM projections

Climate projections from global and regional climate models often need to be corrected due to bias in the models (Xu and Yang 2015; Maraun 2016). For this

Table 1 RCM/GCM combinations: (scenarios RCP 4.5 and RCP 8.5; timeline 2051–2080)

No.	RCM	GCM	Scenario models used in study
1	RCA4 (SMHI)	MPI-ESM-LR	RCA4/MPI-ESM-LR
2	HIRHAM5_V2	ICHEC-EC-EARTH	HIRHAM5_V2/ ICHEC-EC-EARTH
3	CCCLM-4-8-17	MPI-ESM-LR	CCCLM-4-8-17/MPI-ESM-LR
4	RCA4 (SMHI)	CCCma-CanESM2	RCA4/CanESM2

study, the RCMs' projected precipitation and temperature (maximum and minimum) data were corrected using the Q-Q transformation technique. This empirical statistical technique was applied to adjust the statistical distribution of the data from each of the 4 RCMs to match the statistical distribution of the observed data. The Q-Q transformation procedure was applied on a monthly basis on each of the data variables as described by Amadou et al. (2015) and Sarr et al. (2015) as follows:

1. The observed data covering the present horizon was split into two, one half for calibration and the other half for validation. In order to avoid problems related to non-stationarity in hydrologic time series (difficulty in predicting the evolution in time of hydrological processes), the calibration period consisted of every odd year starting from the beginning of the present horizon (i.e., years 1, 3, 5, etc.). The performance of the bias correction was tested on even years (years 2, 4, etc.). The daily time series of the month were extracted for both calibration and validation periods from both observation and RCM projection data.
2. Two empirical cumulative distribution functions, F_{obs} and F_{RCM} , were then developed. F_{obs} was generated using observed data covering the calibration period while the F_{RCM} was generated using the RCM projections for the calibration period.
3. The probability mass function (PMF) of precipitation occurrence (i.e., intensity greater than 1 mm/day) and probability density function (PDF) of precipitation intensity on wet/rainy days and maximum and minimum temperatures were built. The quantile-quantile transformation was applied to produce improved (corrected) future RCM simulations of a variable if it was noticed that the PDF (or PMF) of a corrected variable was closer to the PDF (or PMF) of the observations than the PDF (or PMF) of the raw non-corrected variable.
4. Thus, the bias-corrected RCM projections, X_{CORR} , were generated for the entire period of the uncorrected projection data using the transformation: $X_{\text{CORR}} = F_{\text{obs}}^{-1}(F_{\text{RCM}}(X_{\text{RCM}}))$, where X_{RCM} refers to the uncorrected RCM projection data.

2.2.2 Extreme index calculation

The calculation of indices of climate extremes was conducted using RCLimDex 1.0 software package (Zhang and Yang 2004). In this study, we used indicators devised by the joint World Meteorological Organization Expert Team on Climate Change Detection Indices (ETCCDI). The RCLimDex has a set of 27 indices all of which are temperature and precipitation based. However, not all the indices are applicable/relevant for the African Region. For example, the Iced Days (ID) indices, which measures the annual count when daily maximum temperature is below 0 °C is not applicable in the BVRB. Issues concerning water availability for use are of major concern to the countries sharing the basin, especially Burkina Faso and Ghana. Whereas Ghana depends on the basin for hydro-power generation, Burkina Faso uses the water for irrigation. Also, issue of floods are of major concern in the riparian countries. In the past few decades, the region has recorded significant increases in the frequency of heavy rainfall events (Oyebande and Odunuga 2010), resulting in several instances of water-related disasters. We therefore used only nine of the indices, five temperature-related and four precipitation-related indices (Table 2), that we consider relevant for the study area. The definitions and in-depth description of the indices can be found in Klein Tank et al. (2009) and Zhang et al. (2011). The construction of time series and the extraction of temperature and precipitation indices in RCLimDex are presented in detail by Choi et al. (2009). Data quality control was carried out using the quality control procedure provided in the software.

3 Results and discussion

This section presents the results and discussion of the precipitation and temperature indices considered in the study. The section begins with a brief analysis of the bias correction outputs, followed by the results and discussion of the trends in the observed and projected simulations at the station level. Finally, results of the future projections relative to the baseline period are presented and discussed. The analysis for this part of the study is based on the average of all the 10 stations. In each of the sections, the results of the temperature indices are presented first, followed by that of the precipitation indices.

Table 2 Rainfall and temperature indices used in study

Element	Index	Indicator name	Definition	Units
Rainfall	R99p	Extremely wet days	Annual total PRCP when RR > 99th percentile	mm
Rainfall	CWD	Consecutive wet days	Maximum number of consecutive days with precipitation ≥ 1 mm	days
Rainfall	PRCPTOT	Annual total wet day precipitation	Annual total precipitation in wet days with precipitation ≥ 1 mm	mm
Rainfall	Rx5DAY	Max 5-day precipitation	Annual maximum 5-day precipitation	mm
Tn	Tn10p	Cool night frequency	Percentage of days with TN < 10th percentile	days
Tn	Tn90p	Warm night frequency	Percentage of days with TN > 90th percentile	days
Tx	Tx10p	Cool day frequency	Percentage of days with TX < 10th percentile	days
Tx	Tx90p	Warm day frequency	Percentage of days with TX > 90th percentile	days
Tx	WSDI	Warm spell duration indicator	Annual count of days with at least 6 consecutive days when TX > 90th percentile	days

3.1 Assessment of the model-corrected and model-uncorrected simulations of the observed climate indices

Figure 2 presents the time series of consecutive wet days (CWD) for Bobo-Dioulasso station in the north of the basin in Burkina Faso for the period 1981–2005. The figure was based on observed station data as well as simulated model-corrected and model-uncorrected data of the four models (CCCLM-4-8-17/MPI-ESM-LR, RCA4/CanESM2, RCA4/MPI-ESM-LR, HIRHAM5_V2/ICHEC-EC-EARTH) considered in the study. A quick look reveals the level of biases existing in the model outputs. Among other issues a key consequence of not bias correcting RCM outputs includes inaccurate and unreliable extreme value analysis (Durman et al. 2001). Authors such as Marinucci and Giorgi (1992), Chen et al. (1999) and Murphy (1999) have stressed on the need to improve RCM model outputs prior to their use in impact studies. As shown in our results, the uncorrected RCM outputs highly overestimated the observed CWD. It must be noted, however, that in spite of the correction, a few biases still existed in the model simulations, leading to slight overestimations and underestimations. In Fig. 2a for example, the corrected data is seen to underestimate the CWD for 1989 and overestimate that for the year 1996 and from the years 2000 to 2005. In general, the biases shown in the corrected RCM outputs were much less than the ones by the uncorrected data. While the level of overestimation observed in the corrected model simulations ranged from 4.7 to 26.6%, that in the uncorrected model ranged from 154.7 to 272.7% as shown by the PBIAS in Table 3. Comparison between the RMSE values in the bias-corrected and uncorrected model simulations also shows that a better agreement with the observations was achieved after bias correction, establishing the importance of bias correction in impact studies.

3.2 Trends in present-day climate (1981–2010)

3.2.1 Present-day temperature-based indices (TN10p, TN90p, TX10p, TX90p, WSDI)

Trend analysis and statistics of present-day temperature indices at the 10 stations considered for analysis (Table 4) showed mostly increasing trends in the number of warm days (TX90p), warm nights (TN90p) and warm spells (WSDI) over the BVRB during the 1981–2010 period. The increasing trends in TN90p were statistically significant at 80% of the stations. With regard to the TX90p, 50% of the increasing trends at the stations (mostly in Burkina Faso) were significant. As for the WSDI, none of the increasing trends was statistically significant. The results indicate that the basin (mostly the northern half) got warmer during the analysis period. Trends computed for the cool days (TX10p) and cool nights (TN10p) showed mostly decreases, observed at nine of the stations. The decreasing trends were significant at about 50% of stations, located mostly in the northern half of the basin. This pattern of warming in daytime and nighttime temperatures is similar to that observed in Nigeria during the 1971–2012 period (Abatan et al. 2016). Results of the study by New et al. (2006) also showed increases in both daytime and nighttime hot extremes the West African region over the period 1961–2000. Another study by Mouhamed et al. (2013) suggested a general warming trend throughout the West African Sahel region from 1960 to 2010. Several extreme precipitation and temperature-related studies conducted in Africa (e.g., New et al. 2006; Mekasha et al. 2014; Kruger and Sekele 2013) also indicated decreases in cold extremes and increases in warm extremes. Our study results show that the warming in the BVRB during the 1981–2010 period was more in Burkina Faso than in Ghana.

Fig. 2 Time series of CWD for station Bobo-Dioulasso developed from (i) observed data, (ii) bias-corrected model data for rcp4.5 and (iii) uncorrected model data for rcp4.5: **a** model CCCLM-4-8-17/MPI-ESM-LR, **b** model RCA4/CanESM2, **c** model RCA4/MPI-ESM-LR and **d** model HIRHAM5_V2/ICHEC-EC-EARTH



3.2.2 Present-day precipitation-based indices (R99P, CWD, PRCPOT, RX5DAY)

Table 5 shows trends and significance in present-day extreme climate precipitation indices for the 10 stations. The result showed a general increasing trend in extremely wet days (R99P), annual total wet day precipitation (PRCPTOT) and maximum 5-day precipitation amount (Rx5day). The consecutive wet day index (CWD) on the other hand, exhibited a mix of increasing and decreasing trends. Generally, only a small fraction of the trends in the stations were significant for any of the precipitation indices. The results suggest increases in precipitation intensities and amounts over the basin. Alexander et al. (2006) found that averaged across the globe, extreme precipitation events have been increasing during the 1951–2003 period. Although findings of Mouhamed et al. (2013) showed a general tendency of decreased annual total rainfall for the West African Sahel and for Burkina Faso in particular during 1961–2010, increasing trends of cumulated rainfall of extremely wet days and maximum number of consecutive wet days were observed in their study for the late 1980s. A study by Sarr (2011) also showed that extreme rainfall events became more frequent in the West African Sahel during the last decade, compared to the 1961–1990 period.

3.3 Trends in future climate (2051–2080)

3.3.1 Future temperature-based indices (TN10p, TN90p, TX10p, TX90p, WSDI)

The results of future (2051–2080) trends in extreme temperature indices as projected by the model scenarios are presented in Tables 6, 7, 8 and 9 respectively. The models projected warming in most parts of the stations for the late twenty-first century under both RCP scenarios in agreement with the latest IPCC (2013) report. As depicted in the tables, three (CCCLM-4-8-17/MPI-ESM-LR, RCA4/CanESM2, RCA4/MPI-ESM-LR) of the RCMs projected mostly decreases in the number of cold nights (TN10p) and cold days (TX10p) at each of the 10 stations, and showed mostly increasing trends in the number of warm days (TX90p), warm nights (TN90p) and warm spells (WSDI) for the late twenty-first century under the RCP4.5 scenario. All the models also agreed in their projections of the warming up of the region under the RCP8.5 scenario, showing increases in the hot indices and decreases in the cold indices. Whereas the warming trends projected were mostly statistically significant (except for the WSDI) under the high emission RCP8.5 scenario, that recorded under the RCP4.5 scenarios were mostly insignificant at the 95% confidence level.

Table 3 Scores of bias-corrected and uncorrected RCM model simulations of historical (1981–2005) CWD index at station Bobo-Dioulasso

Model scenarios	Root mean square error		Percent bias (%)	
	Corrected	Uncorrected	Corrected	Uncorrected
CCCLM-4-8-17/MPI-ESM-LR	3.44	8.75	– 26.56	– 154.69
RCA4/CanESM2	2.55	15.25	– 11.72	– 272.66
RCA4/MPI-ESM-LR	3.09	13.59	– 19.53	– 251.56
HIRHAM5_V2/ICHEC-EC-EARTH	2.76	10.13	– 4.69	– 169.53

3.3.2 Future precipitation-based indices (R99P, CWD, PRCPTOT, RX5DAY)

The results of trend analysis and statistics of precipitation-based indices for the BVBR during the late twenty-first century are presented in Tables 10, 11, 12 and 13. Unlike the temperature extremes, trends in the precipitation extremes were highly variable among the RCMs. As noted by several authors (e.g., Orłowsky and Seneviratne 2011; Allen and Ingram 2002) simulations of future precipitation and extreme precipitation analysis are generally associated with high uncertainty levels. With the exception of a projected increase in R99p (RCP4.5 scenario) at majority of the climate stations by three of the RCMs, the trends in the other indices at the various stations were mostly split among the models offering no clear indication of the direction of change. This was the case for the consecutive wet days, total annual precipitation and maximum 5-day rainfall events. Similar to the results obtained under the RCP4.5 scenario, the trend results of the indices under the RCP8.5 scenario were also mostly split among the models and not statistically significant. Three of the RCMs suggested decreases (mostly statistically insignificant) in the consecutive wet day index at most of the analysed stations.

Extreme precipitation analysis for the West Africa region by Sylla et al. (2016) also projected decreases in very wet day intensities in most areas in the region, particularly the areas along the Gulf of Guinea during the mid and end of the twenty-first century under the RCP4.5 scenario. Results of the trend analysis in the other indices CWD, PRCPTOT and RX5day showed no clear trends as the result were split among the models.

3.4 Projected changes in extreme climate indices in the BVRB

Projected changes in temperature and precipitation extremes across the BVRB for the future period (2051–2080) relative to the observed period (1981–2010) are shown in Figs. 3, 4 and 5. Figure 3 presents the percentage change in the extremes as projected by the multi-model ensemble mean RCMs for the average of the 10 stations while Figs. 4 and 5 present the time series analysis. Studies by Paeth et al. (2011) and Nikulin et al. (2012) for example have demonstrated that multi-model ensemble mean RCMs generally perform better than individual models. For this reason, we discuss the changes in the extreme indices with reference to the multi-model ensemble averages.

Table 4 Slopes of trends and associated *p* values of present-day temperature-based indices. Italicized numbers represent trends which are statistically significant at 95% level ($p < 0.05$)

Station name	Tn10p	Tn90p	Tx10p	Tx90p	WSDI
Dedougou	– 0.27 (0.01)	0.22 (0.02)	– 0.33 (0.00)	0.53 (0.00)	0.24 (0.09)
Boromo	– 0.33 (0.00)	0.43 (0.00)	– 0.20 (0.00)	0.25 (0.01)	0.13 (0.19)
Hounde	– 0.33 (0.00)	0.43 (0.00)	– 0.20 (0.00)	0.25 (0.01)	0.13 (0.19)
Bobo-Dioulasso	– 0.19 (0.02)	0.33 (0.00)	– 0.25 (0.00)	0.41 (0.00)	0.18 (0.10)
Gaoua	– 0.07 (0.33)	0.33 (0.00)	– 0.13 (0.08)	0.12 (0.23)	– 0.15 (0.26)
Wa	– 0.24 (0.04)	0.38 (0.02)	– 0.18 (0.01)	0.30 (0.01)	0.11 (0.36)
Batie	– 0.07 (0.33)	0.33 (0.00)	– 0.13 (0.08)	0.12 (0.23)	– 0.15 (0.25)
Bole	– 0.13 (0.15)	0.34 (0.01)	– 0.16 (0.01)	0.22 (0.08)	0.09 (0.56)
Bui	0.04 (0.53)	– 0.24 (0.02)	0.36 (0.08)	0.23 (0.26)	0.18 (0.35)
Wenchi	– 0.01 (0.97)	0.10 (0.52)	– 0.12 (0.16)	0.09 (0.64)	– 0.09 (0.68)
Number of stations with positive trend	1	9	1	10	7
Number of stations with negative trend	9	1	9	0	3

Table 5 Slopes of trends and associated p values of present-day precipitation-based indices. Italicized numbers represent trends which are statistically significant at 95% level ($p < 0.05$)

Station name	R99	CWD	PRCPTOT	Rx5DAY
Dedougou	1.55(0.23)	<i>0.07</i> (0.02)	<i>7.17</i> (0.01)	<i>1.29</i> (0.01)
Boromo	0.39 (0.81)	0.05 (0.19)	4.48 (0.15)	1.09 (0.12)
Houunde	0.17 (0.92)	<i>0.06</i> (0.03)	-1.63 (0.61)	0.45 (0.49)
Bobo-Dioulasso	0.05 (0.97)	-0.02 (0.64)	0.79 (0.81)	0.28 (0.71)
Gaoua	0.17 (0.92)	-0.01 (0.88)	4.68 (0.16)	0.03 (1.00)
Wa	2.09 (0.44)	0.04 (0.34)	8.99 (0.09)	2.27 (0.09)
Batie	1.28 (0.51)	0.01 (0.63)	0.58 (0.87)	0.01 (0.99)
Bole	0.56 (0.81)	-0.00 (0.97)	0.66 (0.86)	0.09 (0.88)
Bui	2.23 (0.22)	-0.03 (0.48)	1.96 (0.69)	-0.10 (0.91)
Wenchi	2.53 (0.32)	0.10 (0.07)	14.88 (0.09)	1.85 (0.10)
Number of stations with positive trend	10	6	9	9
Number of stations with negative trend	0	4	1	1

Compared to the observed period, the percentage of cool nights and days (TN10p and TX10p) and warm nights and days (N90p and TX90p) are expected to be lower during the late 21st under both RCP4.5 and RCP8.5 scenarios (Fig. 3a). The decreases projected are higher in the RCP8.5 scenarios than in the RCP4.5 scenarios. For example, TN90p is projected to range between 3 and 18 days/year under the RCP4.5 scenario (representing a decrease of approximately 41%) and between 1 and 10 days/year (representing a decline of about 65%) under the RCP8.5 scenario (4c). Average future cool days (TX10p) are expected to be more or less the same in comparison with the observed period under the RCP4.5 scenario and decrease slightly (about 1%) under the RCP8.5 scenario (Fig. 3a). In line with our findings, Sillmann et al. (2013) projected a consistent decrease in TN10p and TX10p in tropical regions from the late 20th through to the twenty-first century. Contrary to our findings however, their study projected increases in warm nights and days. Our study projects an increase in warm spells (WSDI under the RCP4.5 scenario and a decrease under the RCP8.5 scenario (Fig. 3a). Future consecutive wet days (CWD) and maximum 5-day precipitation amounts (RX5Day) are expected to increase in comparison with present-day precipitation extremes (Fig. 3b). The projected future CWD ranges between 5 and 6 days/year under both RCP4.5 and RCP8.5 scenarios (Fig. 5b). For the RX5Day, the range is between 124 and 171 mm/year under the RCP4.5 scenario, and between 120 and 148 mm/year under the RCP8.5 scenario (Fig. 5d). The future R99p is expected to be lower than the observed (Fig. 3b) and oscillate between 27 and 109 mm/year under the RCP4.5 scenario and between 25 and 72 mm/year under the RCP8.5 scenario (Fig. 5a). In agreement with our findings, Sylla et al. (2016) observed that most West African countries will experience small decreases in very wet day intensity under the RCP 4.5 scenario for the late and end of the twenty-first century. Future PRCPTOT is projected to increase (decrease) by about 1%

under the RCP8.5 (RCP4.5) scenario in comparison with the observed period and range between 810 and 1130 mm/year and between 866 and 1120 mm/year during the late twenty-first century under the RCP4.5 and RCP8.5 scenarios respectively (Fig. 5c). Our results suggest that compared to the observed period, future rainfall duration will increase while the intensity reduces. On the other hand, total rainfall amounts for the future will be similar to the observed period. Similar to our results, previous studies on extreme precipitation events, such as the one by Pinto et al. (2016) indicated a decrease in annual total precipitation and increase in maximum 5-day precipitation amounts in some parts of South Africa during the late to end of twenty-first century relative to the 1976–2005 period.

4 Conclusion

This study analysed the variability and trends of extreme climate events (5 temperature- and 4 precipitation-related) in the BVRB in West Africa for the present (1981–2010) and made projections for the future (2051–2080) using a range of ensemble model outputs.

Results of the study indicated that the Quantile-Quantile (Q-Q) transformation technique was useful in reducing the biases in the ensemble models employed in the study. Analysis of the present-day (1981–2010) precipitation- and temperature-based extreme indices demonstrated increases in the warm indices (TX90p and TN90p) and a decline in the cold indices (TX10p and TN10p). Warm spells also increased over the basin. The analysis indicated that Burkina Faso, located north of the basin, experienced more warming than neighbouring Ghana which is located in the southern portion of the basin. Results of the precipitation analysis suggested an increase in precipitation intensity and amount over the period. The period saw increases in extremely wet days (R99P), maximum 5-day precipitation amount (Rx5day) and annual total

Table 6 Slopes of trends and associated *p* values of future (2051–2080) temperature-based indices under RCP4.5 and RCP8.5 scenarios of the CCCLM-4-8-17/MPI-ESM-LR model. Italicized numbers represent trends which are statistically significant at 95% level (*p* < 0.05)

Station name	Tn10p		Tn90p		Tx10p		Tx90p		WSDI	
	RCP4.5	RCP8.5	RCP4.5	RCP8.5	RCP4.5	RCP8.5	RCP4.5	RCP8.5	RCP4.5	RCP8.5
Dedougou	-0.14 (0.28)	-0.48 (0.00)	0.15 (0.25)	0.18 (0.03)	-0.12 (0.28)	-0.37 (0.00)	0.15 (0.30)	0.18 (0.06)	0.13 (0.37)	0.20 (0.28)
Boromo	-0.16 (0.23)	-0.51 (0.00)	0.11 (0.24)	0.17 (0.05)	-0.09 (0.41)	-0.40 (0.00)	0.16 (0.27)	0.17 (0.08)	0.20 (0.30)	0.10 (0.51)
Hounde	-0.15 (0.24)	-0.54 (0.00)	0.11 (0.28)	0.17 (0.04)	-0.09 (0.38)	-0.45 (0.00)	0.16 (0.27)	0.21 (0.05)	0.3 (0.16)	0.06 (0.73)
Bobo-dioulasso	-0.11 (0.36)	-0.49 (0.00)	0.13 (0.21)	0.16 (0.03)	-0.05 (0.65)	-0.43 (0.00)	0.11 (0.46)	0.12 (0.09)	-0.01 (0.99)	0.06 (0.64)
Gaoua	-0.10 (0.49)	-0.57 (0.00)	0.12 (0.35)	0.16 (0.04)	-0.02 (0.82)	-0.42 (0.00)	0.21 (0.25)	0.23 (0.02)	0.05 (0.73)	0.19 (0.23)
Wa	-0.09 (0.50)	-0.55 (0.00)	0.12 (0.34)	0.16 (0.03)	-0.03 (0.77)	-0.41 (0.00)	0.18 (0.31)	0.22 (0.02)	0.12 (0.52)	0.22 (0.25)
Batie	-0.09 (0.51)	-0.58 (0.00)	0.11 (0.42)	0.18 (0.03)	-0.03 (0.80)	-0.37 (0.00)	0.15 (0.36)	0.24 (0.03)	-0.04 (0.80)	0.16 (0.33)
Bole	-0.09 (0.50)	-0.57 (0.00)	0.08 (0.50)	0.13 (0.03)	-0.01 (0.95)	-0.30 (0.01)	0.13 (0.44)	0.18 (0.03)	0.05 (0.75)	0.12 (0.37)
Bui	-0.05 (0.72)	-0.54 (0.00)	0.09 (0.43)	0.10 (0.07)	0.01 (0.96)	-0.31 (0.02)	0.08 (0.56)	0.02 (0.01)	-0.04 (0.70)	0.07 (0.41)
Wenchi	-0.08 (0.59)	-0.54 (0.00)	0.20 (0.06)	0.12 (0.05)	-0.09 (0.37)	-0.34 (0.01)	0.13 (0.26)	0.22 (0.01)	0.21 (0.25)	0.09 (0.22)
Number of stations with positive trend	0	0	10	10	0	0	10	10	7	10
Number of stations with negative trend	10	10	0	0	10	10	0	0	3	0

Table 7 Slopes of trends and associated p values of future (2051–2080) temperature-based indices under RCP4.5 and RCP8.5 scenarios of the RCA4/CanESM2 model. Italicized numbers represent trends which are statistically significant at 95% level ($p < 0.05$)

Station name	Tn10p		Tn90p		Tx10p		Tx90p		WSDI	
	RCP4.5	RCP8.5	RCP4.5	RCP8.5	RCP4.5	RCP8.5	RCP4.5	RCP8.5	RCP4.5	RCP8.5
Dedougou	-0.13 (0.19)	-0.56 (0.00)	0.13 (0.30)	0.28 (0.00)	-0.12 (0.20)	-0.43 (0.00)	0.09 (0.43)	0.14 (0.01)	0.19 (0.22)	0.05 (0.14)
Boromo	-0.46 (0.00)	-0.61 (0.00)	0.14 (0.01)	0.23 (0.01)	-0.36 (0.00)	-0.45 (0.00)	0.15 (0.00)	0.08 (0.07)	0.07 (0.16)	0.09 (0.03)
Houde	-0.20 (0.10)	-0.67 (0.00)	0.12 (0.29)	0.29 (0.00)	-0.13 (0.19)	-0.45 (0.00)	0.21 (0.10)	0.10 (0.02)	0.15 (0.35)	0.02 (0.54)
Bobo-dioulasso	-0.19 (0.07)	-0.59 (0.00)	-0.19 (0.07)	-0.59 (0.00)	-0.15 (0.11)	-0.50 (0.00)	0.20 (0.11)	0.12 (0.00)	0.4 (0.01)	0.05 (0.15)
Gaoua	0.08 (0.41)	-0.65 (0.00)	-0.07 (0.46)	0.21 (0.00)	0.07 (0.29)	-0.48 (0.00)	-0.08 (0.39)	0.12 (0.02)	-0.13 (0.33)	0.05 (0.19)
Wa	-0.14 (0.16)	-0.57 (0.00)	0.03 (0.75)	0.15 (0.01)	-0.10 (0.31)	-0.47 (0.00)	0.26 (0.03)	0.01 (0.04)	0.23 (0.19)	0.03 (0.15)
Batie	-0.18 (0.15)	-0.70 (0.00)	0.03 (0.69)	0.18 (0.00)	-0.15 (0.11)	-0.54 (0.00)	0.24 (0.30)	0.87 (0.00)	0.15 (0.84)	1.21 (0.00)
Bole	-0.21 (0.11)	-0.50 (0.00)	0.05 (0.57)	0.18 (0.01)	-0.17 (0.07)	-0.5 (0.00)	0.24 (0.02)	0.12 (0.01)	0.26 (0.04)	0.11 (0.03)
Bui	-0.28 (0.03)	-0.47 (0.00)	0.06 (0.41)	0.09 (0.04)	-0.19 (0.06)	-0.57 (0.00)	0.20 (0.00)	0.02 (0.43)	0.17 (0.01)	0.04 (0.09)
Wenchi	-0.31 (0.03)	-0.37 (0.00)	0.02 (0.77)	0.10 (0.03)	-0.18 (0.078)	-0.58 (0.00)	0.13 (0.04)	0.03 (0.12)	0.16 (0.00)	No trend
Number of stations with positive trend	0	0	8	9	0	0	9	10	9	9
Number of stations with negative trend	10	10	2	1	10	10	1	0	1	0

Table 8 Slopes of trends and associated p values of future (2051–2080) temperature-based indices under RCP4.5 and RCP8.5 scenarios of the RCA4/MPI-ESM-LR model. Italicized numbers represent trends which are statistically significant at 95% level ($p < 0.05$)

Station name	Tn10p		Tn90p		Tx10p		Tx90p		WSDI	
	RCP4.5	RCP8.5	RCP4.5	RCP8.5	RCP4.5	RCP8.5	RCP4.5	RCP8.5	RCP4.5	RCP8.5
Dedougou	-0.14 (0.28)	-0.52 (0.00)	0.17 (0.10)	0.286 (0.00)	-0.10 (0.40)	0.42 (0.00)	0.19 (0.12)	0.19 (0.01)	0.03 (0.86)	0.20 (0.07)
Boromo	-0.17 (0.23)	-0.58 (0.00)	0.24 (0.06)	0.256 (0.00)	-0.11 (0.33)	-0.42 (0.00)	0.19 (0.13)	0.24 (0.02)	0.09 (0.69)	0.23 (0.16)
Hounde	-0.16 (0.26)	-0.59 (0.00)	0.21 (0.06)	0.219 (0.00)	-0.12 (0.27)	-0.43 (0.00)	0.21 (0.12)	0.23 (0.02)	0.13 (0.56)	0.21 (0.15)
Bobo-dioulasso	-0.16 (0.25)	-0.57 (0.00)	0.16 (0.05)	0.286 (0.00)	-0.10 (0.36)	-0.46 (0.00)	0.18 (0.10)	0.11 (0.03)	0.20 (0.11)	0.05 (0.17)
Gaoua	-0.17 (0.17)	-0.59 (0.00)	0.03 (0.79)	0.26 (0.00)	-0.11 (0.27)	-0.41 (0.00)	0.21 (0.06)	0.25 (0.00)	0.24 (0.04)	0.18 (0.05)
Wa	-0.19 (0.18)	-0.54 (0.00)	0.12 (0.12)	0.24 (0.00)	-0.11 (0.23)	-0.40 (0.00)	0.14 (0.26)	0.23 (0.00)	0.17 (0.15)	0.17 (0.07)
Batie	-0.14 (0.36)	-0.59 (0.00)	0.13 (0.36)	0.25 (0.00)	-0.09 (0.37)	-0.40 (0.00)	0.17 (0.19)	0.26 (0.001)	0.20 (0.38)	0.16 (0.06)
Bole	-0.14 (0.42)	-0.52 (0.00)	0.10 (0.23)	0.22 (0.00)	-0.11 (0.30)	-0.42 (0.00)	0.19 (0.16)	0.19 (0.00)	0.32 (0.10)	0.09 (0.17)
Bui	-0.08 (0.65)	-0.46 (0.00)	0.10 (0.14)	0.14 (0.00)	-0.01 (0.33)	-0.40 (0.00)	0.13 (0.21)	0.15 (0.00)	0.07 (0.47)	0.01 (0.16)
Wenchi	0.04 (0.64)	-0.67 (0.00)	-0.04 (0.56)	0.12 (0.01)	0.09 (0.199)	-0.38 (0.00)	-0.07 (0.47)	0.09 (0.01)	0.04 (0.70)	0.20 (0.70)
Number of stations with positive trend	0	0	9	10	1	1	9	10	10	10
Number of stations with negative trend	10	10	1	0	9	9	1	0	0	0

Table 9 Slopes of trends and associated p values of future (2051–2080) temperature-based indices under RCP4.5 and RCP8.5 scenarios of the HIRHAM5_V2/ICHEC-EC-EARTH model. Italicized numbers represent trends which are statistically significant at 95% level ($p < 0.05$)

Station name	Tn10p		Tn90p		Tx10p		Tx90p		WSDI	
	RCP4.5	RCP8.5	RCP4.5	RCP8.5	RCP4.5	RCP8.5	RCP4.5	RCP8.5	RCP4.5	RCP8.5
Dedougou	0.14 (0.17)	-0.66 (0.00)	-0.16 (0.16)	0.29 (0.00)	0.10 (0.30)	-0.50 (0.00)	-0.23 (0.07)	0.44 (0.00)	-0.30 (0.06)	0.20 (0.02)
Boromo	0.12 (0.20)	-0.71 (0.00)	-0.16 (0.12)	0.28 (0.00)	0.12 (0.12)	-0.50 (0.00)	-0.23 (0.05)	0.45 (0.00)	-0.27 (0.03)	0.36 (0.01)
Hounde	-0.19 (0.10)	-0.67 (0.00)	0.12 (0.29)	0.24 (0.00)	-0.13 (0.20)	-0.43 (0.00)	0.21 (0.10)	0.40 (0.00)	0.18 (0.23)	0.27 (0.02)
Bobo-dioulasso	0.07 (0.41)	-0.64 (0.00)	-0.10 (0.21)	0.26 (0.00)	0.08 (0.25)	-0.40 (0.00)	-0.16 (0.13)	0.41 (0.00)	-0.19 (0.22)	0.19 (0.03)
Gaoua	-0.23 (0.16)	-0.60 (0.00)	0.15 (0.07)	0.12 (0.01)	-0.14 (0.19)	-0.35 (0.00)	0.13 (0.29)	0.37 (0.00)	0.15 (0.40)	0.16 (0.05)
Wa	0.06 (0.52)	-0.60 (0.00)	-0.08 (0.32)	0.13 (0.00)	0.08 (0.22)	-0.32 (0.00)	-0.07 (0.46)	0.36 (0.00)	-0.18 (0.27)	0.15 (0.09)
Batie	0.05 (0.53)	-0.76 (0.00)	-0.09 (0.30)	0.17 (0.00)	0.10 (0.12)	-0.41 (0.00)	-0.04 (0.69)	0.44 (0.00)	-0.11 (0.37)	0.41 (0.00)
Bole	0.09 (0.30)	-0.79 (0.00)	-0.08 (0.23)	0.12 (0.00)	0.13 (0.06)	-0.44 (0.00)	-0.04 (0.65)	0.44 (0.00)	-0.11 (0.43)	0.31 (0.00)
Bui	0.07 (0.44)	-0.80 (0.00)	-0.06 (0.43)	0.10 (0.00)	0.09 (0.18)	-0.48 (0.00)	-0.05 (0.55)	0.36 (0.00)	0.07 (0.53)	0.05 (0.32)
Wenchi	-0.05 (0.75)	-0.88 (0.00)	0.07 (0.50)	0.12 (0.02)	0.08 (0.47)	-0.51 (0.00)	0.10 (0.56)	0.34 (0.00)	0.03 (0.79)	0.16 (0.04)
Number of stations with positive trend	7	0	3	10	8	0	3	10	4	10
Number of stations with negative trend	3	10	7	0	2	10	7	0	6	0

Table 10 Slopes of trends and associated *p* values of future (2051–2080) precipitation-based indices under RCP4.5 and RCP8.5 scenarios of the CCCLM-4-8-17/MPI-ESM-LR model. Italicized numbers represent trends which are statistically significant at 95% level ($p < 0.05$)

Station name	R99		CWD		PRCPTOT		Rx5DAY	
	RCP4.5	RCP8.5	RCP4.5	RCP8.5	RCP4.5	RCP8.5	RCP4.5	RCP8.5
Dedougou	-0.17 (0.90)	-0.20 (0.80)	0.02 (0.54)	-0.02 (0.45)	-3.76 (0.36)	0.48 (0.88)	-0.42 (0.62)	0.03 (0.96)
Boromo	-2.19 (0.07)	-0.05 (0.96)	0.06 (0.08)	-0.02 (0.58)	-3.89 (0.33)	-0.42 (0.89)	-0.58 (0.49)	-0.50 (0.39)
Hounde	-1.26 (0.18)	0.67 (0.43)	0.04 (0.152)	-0.02 (0.31)	-5.90 (0.17)	-1.74 (0.60)	-0.55 (0.36)	-0.41 (0.55)
Bobo-dioulasso	0.23 (0.85)	1.37 (0.22)	-0.03 (0.35)	-0.06 (0.08)	-5.44 (0.25)	-3.87 (0.40)	-0.02 (0.98)	0.28 (0.72)
Gaoua	-0.34 (0.79)	-1.80 (0.28)	0.01 (0.64)	-0.05 (0.15)	-4.11 (0.39)	-8.41 (0.03)	0.12 (0.89)	-1.09 (0.14)
Wa	-2.01 (0.23)	-2.88 (0.09)	0.01 (0.96)	-0.04 (0.17)	-5.75 (0.27)	-8.62 (0.04)	-0.41 (0.61)	-1.84 (0.03)
Batie	-4.74 (0.01)	-2.02 (0.29)	-0.01 (0.97)	-0.03 (0.50)	-7.62 (0.15)	-5.09 (0.21)	-1.63 (0.12)	-0.33 (0.72)
Bole	-1.21 (0.54)	0.94 (0.61)	-0.01 (0.75)	-0.06 (0.24)	-5.52 (0.28)	-0.44 (0.92)	-2.20 (0.01)	0.14 (0.90)
Bui	-3.12 (0.08)	0.17 (0.91)	-0.08 (0.21)	-0.07 (0.21)	-5.79 (0.32)	-5.03 (0.33)	-1.74 (0.11)	0.82 (0.34)
Wenchi	-0.14 (0.94)	0.26 (0.88)	0.05 (0.04)	-0.07 (0.15)	5.11 (0.30)	-3.66 (0.39)	0.76 (0.31)	-3.66 (0.39)
Number of stations with positive trend	1	5	6	0	1	1	2	4
Number of stations with negative trend	9	5	4	10	9	9	8	6

Table 11 Slopes of trends and associated p values of future (2051–2080) precipitation-based indices under RCP4.5 and RCP8.5 scenarios of the RCA4/CanESM2 model. Italicized numbers represent trends which are statistically significant at 95% level ($p < 0.05$)

Station name	R99		CWD		PRCPTOT		Rx5DAY	
	RCP4.5	RCP8.5	RCP4.5	RCP8.5	RCP4.5	RCP8.5	RCP4.5	RCP8.5
Dedougou	0.82 (0.48)	No trend	-0.01 (0.71)	0.02 (0.57)	-0.30 (0.92)	4.66 (0.19)	1.07 (0.18)	1.56 (0.08)
Boromo	1.33 (0.45)	-0.04 (0.98)	-0.03 (0.43)	0.09 (0.04)	-7.23 (0.18)	6.46 (0.09)	-1.07 (0.12)	2.10 (0.03)
Houde	0.96 (0.51)	No trend	-0.08 (0.01)	0.08 (0.10)	-3.97 (0.31)	11.31 (0.01)	1.06 (0.14)	2.71 (0.01)
Bobo-dioulasso	0.49 (0.66)	1.37 (0.22)	0.01 (0.78)	-0.06 (0.08)	-2.88 (0.44)	-3.87 (0.36)	-0.39 (0.56)	0.28 (0.72)
Gaoua	-1.84 (0.36)	-0.23 (0.87)	0.01 (0.71)	0.05 (0.29)	1.57 (0.71)	0.82 (0.85)	-0.00 (0.96)	0.35 (0.67)
Wa	3.17 (0.12)	4.11 (0.10)	-0.03 (0.58)	0.07 (0.25)	-3.44 (0.49)	6.53 (0.21)	1.83 (0.13)	1.32 (0.15)
Batie	-4.74 (0.01)	0.91 (0.57)	-0.00 (0.97)	0.24 (0.05)	-7.62 (0.15)	9.16 (0.09)	-1.63 (0.12)	1.91 (0.035)
Bole	1.12 (0.70)	-0.55 (0.77)	0.02 (0.59)	-0.04 (0.28)	-4.13 (0.39)	3.58 (0.42)	-0.35 (0.81)	0.65 (0.55)
Bui	-2.08 (0.16)	No trend	-0.03 (0.45)	-0.01 (0.9)	-6.73 (0.21)	9.02 (0.05)	-0.14 (0.92)	2.34 (0.02)
Wenchi	4.39 (0.04)	2.20 (0.31)	-0.06 (0.246)	-0.04 (0.32)	1.26 (0.82)	3.32 (0.49)	2.27 (0.02)	0.38 (0.62)
Number of stations with positive trend	7	4	4	6	3	9	4	10
Number of stations with negative trend	3	3	6	4	7	1	6	0

Table 12 Slopes of trends and associated p values of future (2051–2080) precipitation-based indices under RCP4.5 and RCP8.5 scenarios of the RCA4/MPI-ESM-LR model. Italicized numbers represent trends which are statistically significant at 95% level ($p < 0.05$)

Station name	R99		CWD		PRCPTOT		Rx5DAY	
	RCP4.5	RCP8.5	RCP4.5	RCP8.5	RCP4.5	RCP8.5	RCP4.5	RCP8.5
Dedougou	1.02 (0.32)	1.70 (0.26)	0.06 (0.20)	0.02 (0.50)	-3.43 (0.40)	-3.17 (0.39)	0.73 (0.40)	0.13 (0.86)
Boromo	1.52 (0.30)	0.05 (0.97)	0.00 (0.95)	0.02 (0.52)	-4.47 (0.34)	-5.52 (0.06)	0.21 (0.81)	0.77 (0.06)
Hounde	0.87 (0.59)	0.45 (0.71)	-0.03 (0.41)	-0.96 (0.08)	-1.30 (0.77)	-6.12 (0.13)	0.36 (0.71)	-0.74 (0.34)
Bobo-dioulasso	0.75 (0.59)	-0.08 (0.93)	-0.10 (0.01)	-0.02 (0.56)	-2.63 (0.65)	-4.83 (0.283)	0.23 (0.81)	-0.37 (0.63)
Gaoua	0.93 (0.546)	-1.05 (0.61)	-0.02 (0.63)	-0.01 (0.40)	-0.19 (0.96)	-1.84 (0.67)	-0.60 (0.57)	-0.60 (0.57)
Wa	0.65 (0.78)	0.93 (0.55)	-0.01 (0.78)	-0.08 (0.14)	3.45 (0.56)	-7.57 (0.11)	1.61 (0.18)	-1.32 (0.18)
Batie	6.93 (0.00)	-0.08 (0.93)	-0.03 (0.51)	-0.02 (0.56)	3.758 (0.53)	-4.83 (0.28)	3.32 (0.02)	-0.37 (0.63)
Bole	6.40 (0.00)	-1.19 (0.57)	-0.02 (0.54)	-0.06 (0.05)	3.72 (0.52)	-13.15 (0.03)	2.01 (0.09)	-1.82 (0.13)
Bui	1.97 (0.26)	1.33 (0.45)	0.04 (0.34)	-0.03 (0.43)	4.96 (0.31)	-7.23 (0.17)	0.48 (0.56)	-1.07 (0.12)
Wenchi	-0.90 (0.60)	0.42 (0.83)	-0.04 (0.60)	-0.04 (0.32)	-1.24 (0.79)	-0.39 (0.93)	1.25 (0.16)	-0.67 (0.45)
Number of stations with positive trend	9	6	4	2	4	0	9	2
Number of stations with negative trend	1	4	6	8	6	10	1	8

Table 13 Slopes of trends and associated p values of future (2051–2080) precipitation-based indices under RCP4.5 and RCP8.5 scenarios of the HIRHAM5_V2/ICHEC-EC-EARTH model. *Italicized numbers represent trends which are statistically significant at 95% level ($p < 0.05$)*

Station name	R99		CWD		PRCPTOT		Rx5DAY	
	RCP4.5	RCP8.5	RCP4.5	RCP8.5	RCP4.5	RCP8.5	RCP4.5	RCP8.5
Dedougou	1.26 (0.33)	0.29 (0.86)	-0.01 (0.83)	-0.03 (0.29)	1.64 (0.61)	1.17 (0.78)	0.21 (0.72)	0.15 (0.87)
Boromo	1.87 (0.25)	-1.84 (0.25)	-0.01 (0.98)	-0.02 (0.59)	2.61 (0.41)	0.23 (0.96)	1.22 (0.07)	-1.03 (0.25)
Houde	0.96 (0.51)	1.02 (0.36)	-0.08 (0.01)	-0.01 (0.78)	-3.97 (0.31)	4.07 (0.36)	1.06 (0.14)	0.24 (0.81)
Bobo-dioulasso	2.60 (0.07)	-0.26 (0.89)	-0.04 (0.17)	0.01 (0.73)	0.72 (0.85)	3.02 (0.48)	<i>1.89</i> (0.01)	2.02 (0.05)
Gaoua	<i>6.45</i> (0.00)	-1.05 (0.61)	-0.01 (0.65)	-0.03 (0.04)	6.65 (0.24)	-1.84 (0.67)	3.74 (0.01)	0.47 (0.62)
Wa	-1.94 (0.24)	-1.01 (0.24)	-0.01 (0.63)	-0.01 (0.65)	-0.12 (0.97)	-1.78 (0.70)	-0.30 (0.65)	-0.65 (0.41)
Batie	1.65 (0.41)	-1.91 (0.31)	-0.023 (0.35)	-0.02 (0.48)	4.49 (0.14)	-2.03 (0.70)	-0.05 (0.96)	0.01 (0.99)
Bole	2.20 (0.38)	0.58 (0.83)	0.01 (0.76)	<i>0.05</i> (0.04)	5.55 (0.16)	-0.53 (0.91)	0.91 (0.50)	-0.16 (0.87)
Bui	2.85 (0.14)	0.98 (0.62)	-0.02 (0.43)	-0.01 (0.94)	-0.56 (0.91)	4.30 (0.46)	0.81 (0.36)	-1.18 (0.24)
Wenchi	-2.50 (0.08)	-0.04 (0.96)	-0.04 (0.60)	<i>0.04</i> (0.04)	-1.34 (0.82)	2.16 (0.70)	-1.49 (0.24)	-0.67 (0.55)
Number of stations with positive trend	8	4	1	3	6	6	7	5
Number of stations with negative trend	2	6	9	7	4	4	3	5

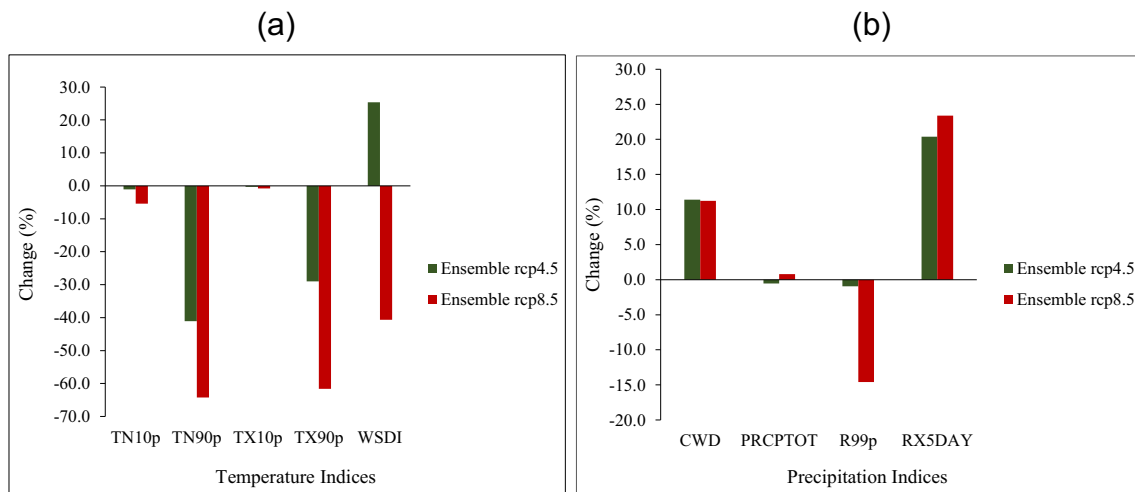


Fig. 3 Percentage change in temperature and precipitation extremes relative to the observed period **a** temperature indices and **b** precipitation indices

wet day precipitation (PRCPTOT). No clear trends were observed for the consecutive wet day index (CWD) as the analysis showed a mix of increasing and decreasing trends.

Increases in warm extremes over the basin is projected for the late twenty-first century under both RCP4.5 and RCP8.5 scenarios. Majority (3 out of 4) of the ensemble models projected decreasing trends in the cold indices (TX10p and TN10p) and increasing trends in the warm indices (TX90p and TN90p). The models offered no clear indication on the direction of change in CWD, PRCPTOT and RX5day as the

trend results mostly showed a mix of positive and negative trends. An increase in extremely wet day events (R99p) is however projected by majority of the model ensembles.

Relative to the observed period, a decrease in both cold (TX10p and TN10p) and warm (TX90p and TN90p) extremes is projected for the late twenty-first century under both RCP4.5 and RCP8.5 scenarios, indicating that the basin will experience less of cold and warm extremes in comparison to the observed period. The decline is projected to be more pronounced under the RCP8.5 scenario than under the RCP4.5

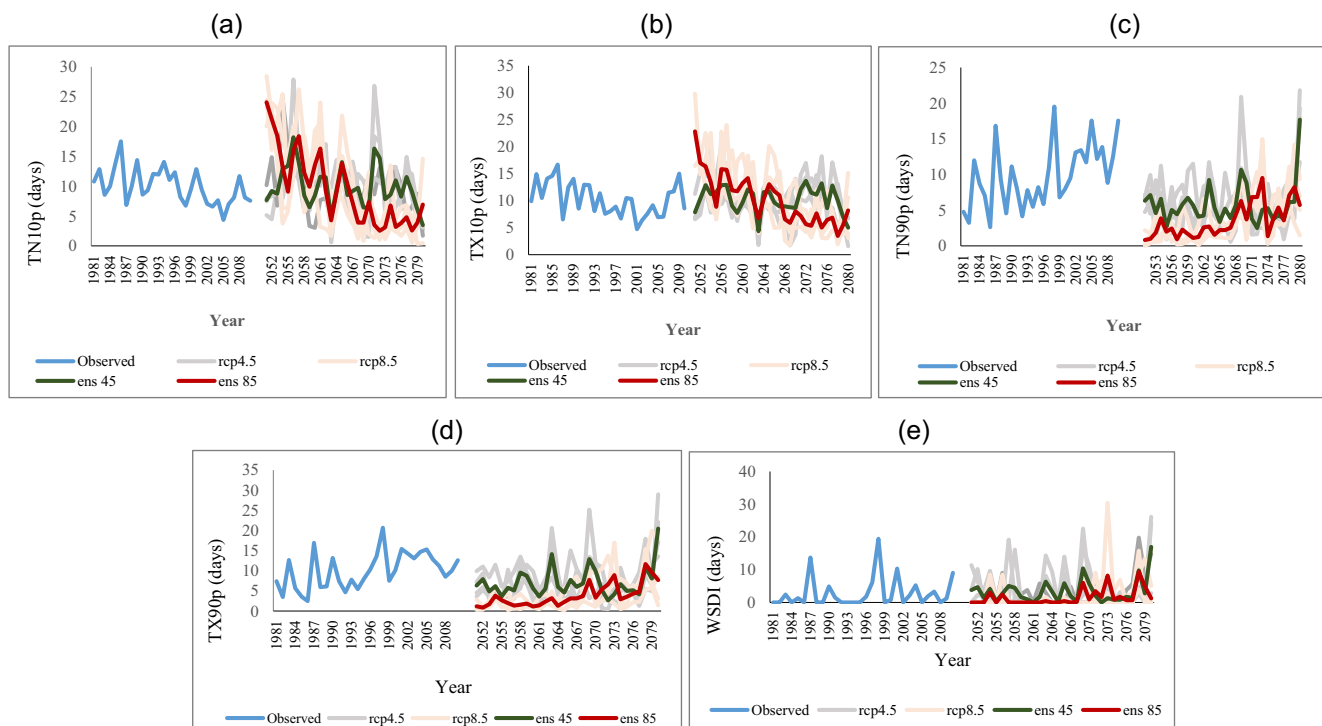


Fig. 4 Time series of future temperature-related indices: **a** number of cool nights (TN10p), **b** number of cool days (TX90p), **c** number of warm nights (TN90p), **d** number of warm days (TX90p) and **e** warm spells (WSDI) in the Black Volta Basin for the period 2051–2080. The blue line

represents the observation; the grey and orange lines represent outputs of the four models under the rcp4.5 and rcp8.5 scenarios, respectively; the green and red lines represent the ensemble of the RCMs under the rcp4.5 and rcp8.5 scenarios, respectively

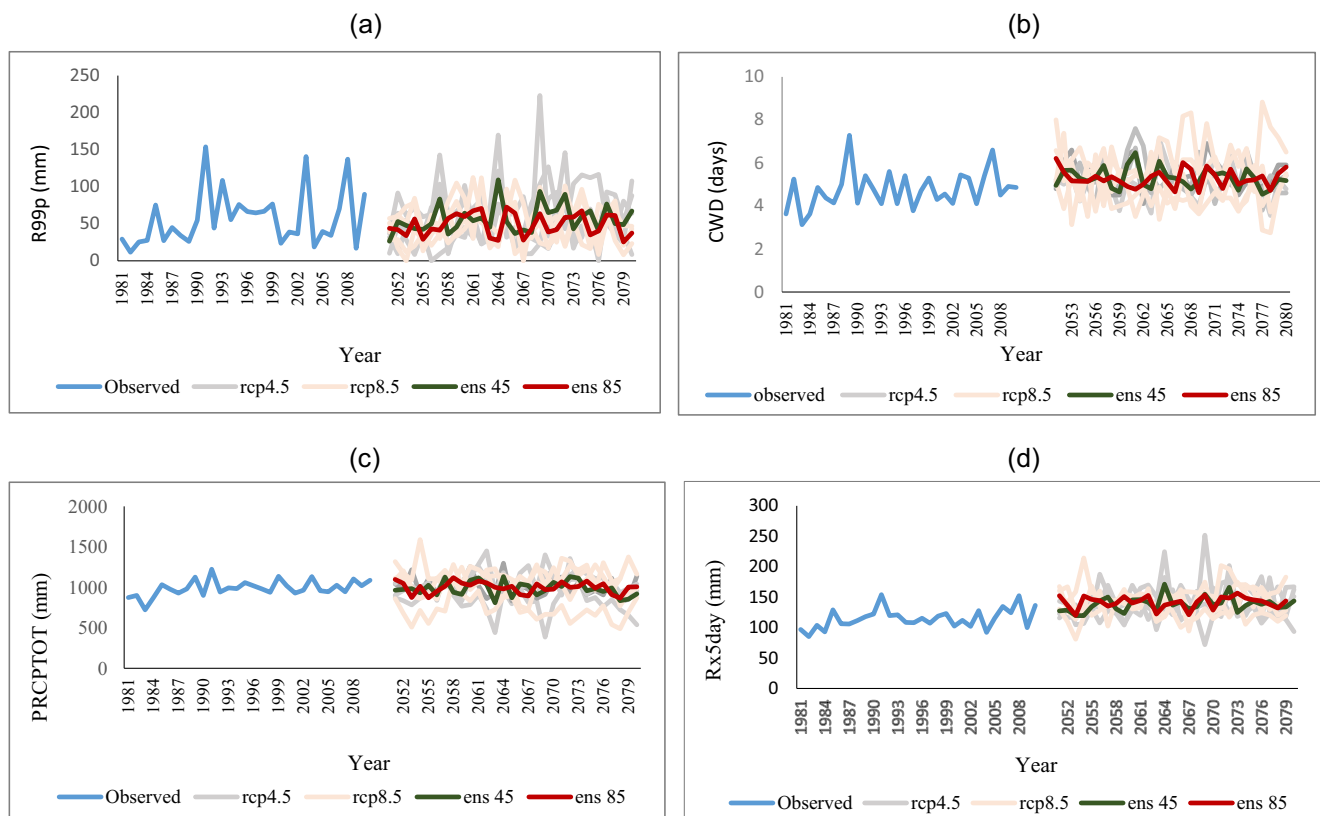


Fig. 5 Time series of future precipitation-related indices: **a** extremely wet days (R99P), **b** consecutive wet days (CWD), **c** annual total wet day precipitation (PRCPTOT) and **d** maximum 5-day precipitation amount (Rx5day) in the Black Volta Basin for the period 2051–2080. The blue

line represents the observation; the grey and orange lines represent outputs of the four models under the rcp4.5 and rcp8.5 scenarios, respectively; the green and red lines represent the ensemble of the RCMs under the rcp4.5 and rcp8.5 scenarios, respectively

scenario. Warm spells are expected to be more under the RCP4.5 scenario and less under the RCP8.5 scenario. Consecutive wet days (CWD) and maximum 5-day precipitation amounts (RX5Day) are expected to increase under both RCP scenarios in comparison with observations of the observed period. Extremely wet day events (R99p) are expected to be less in the future compared with the observed, with the reduction being higher under the RCP8.5 scenario than under the RCP4.5 scenario. The total annual precipitation (PRCPTOT) for the future is projected to vary slightly in comparison with observed period. The precipitation amount is expected to decrease by about 1% under the RCP4.5 scenario and increase by a similar percentage under the RCP8.5 scenario. As previously discussed, the results of this study will help in exploring opportunities for managing the risks of weather- and climate-related disasters in the BVRB.

Acknowledgements The authors would like to thank the German Federal Ministry of Education and Research (BMBF) for providing the funds for this research through the West African Science Service Centre on Climate Change and Adapted Land Use (WASCAL; www.wascal.org). Thanks to Dr. Osumane Seidou of the University of Ottawa, Canada, for providing the CORDEX data used in this study. Our thanks also go to the Meteorological Agencies in Ghana and Burkina Faso for providing the observed meteorological data for the Black Volta Basin.

References

- Abatan AA, Abiodun BJ, Lawal KA, Gutowski WJ (2016) Trends in extreme temperature over Nigeria from percentile-based threshold indices. *Int J Climatol* 36:2527–2540. <https://doi.org/10.1002/joc.4510>
- Abiodun BJ, Lawal KA, Salami AT, Abatan AA (2013) Potential influences of global warming on future climate and extreme events in Nigeria. *Reg Environ Chang* 13(3):477–491
- Alexander LV, Zhang X, Peterson T, Caesar J, Gleason B, Klein Tank AMG, Haylock M, Collins D, Trewin B, Rahimzadeh F, Tagipour A, Kumar Kolli R, Revadekar JV, Griffiths G, Vincent L, Stephenson DB, Burn J, Aguilar E, Brunet M, Taylor M, New M, Zhai P, Rusticucci M, Vazquez Aguirre JL (2006) Global observed changes in daily climate extremes of temperature and precipitation. *J Geophys Res-Atmos* 111:D05109
- Allen MR, Ingram WJ (2002) Constraints on future changes in climate and the hydrologic cycle. *Nature* 419(6903):224–232
- Amadou A, Abdouramane G, Seidou O, Seidou Sanda I (2015) Changes to flow regime on the Niger River at Koulikoro under a changing climate. *Hydrol Sci J* 60(10):1709–1723
- Barry B, Obuobie E, Andreini M, Andah W, Pluquet M (2005) The Volta River Basin; comprehensive assessment of water management in agriculture, International Water Management Institute
- Boko M, Niang I, Nyong A, Vogel C, Githeko A, Medany M, Osman-Elasha B, Tabo R, Yanda P (2007) Climate Change 2007: Impacts, Adaptation and Vulnerability. Chapter 9: Africa. In: Parry ML, Canziani OF, Palutikof JP, van der Linden PJ, Hanson CE (eds)

- Contribution of Working Group II to the Fourth Assessment Report of the Intergovernmental Panel on Climate Change. Cambridge University Press, UK, Cambridge, pp 433–467
- Chen S-C, Roads JO, Juang H-MH, Kanamitsu M (1999) Global to regional simulations of California wintertime precipitation. *J Geophys Res* 104(D24):31,517–31,532. <https://doi.org/10.1029/1998JD200043>
- Choi G, Collins D, Ren G, Trewin B, Baldi M, Fukuda Y, Afzaal M, Pianmana T, Gomboluudev P, Thi Thanh Huong P, Lias N, Kwon W-T, Boo K-O, Cha Y-M, Zhou Y (2009) Changes in means and extreme events of temperature and precipitation in the Asia-Pacific network region, 1955–2007. *Int J Climatol* 29(1):1906–1925
- Climate and Development Knowledge Network (CDKN) 2014 The IPCC's Fifth Assessment Report: What's in it for Africa? <http://cdkn.org/resource/highlights-africa-ar5/>. 14 August 2015.
- Dosio A, Panitz HJ, Schubert-Frisius M, Lüthi D (2015) Dynamical downscaling of CMIP5 global circulation models over CORDEX-Africa with COSMO-CLM: evaluation over the present climate and analysis of the added value. *Clim Dyn* 44:2637–2661
- Durman C, Gregory J, Kassell D, Jones R, Murphy J (2001) A comparison of extreme European daily precipitation simulated by a global and a regional climate model for present and future climates. *Q J R Meteorol Soc* 127:1005–1015. <https://doi.org/10.1002/qj.49712757316>
- Endris HS, Lennard C, Hewitson B, Dosio A, Nikulin G, Panitz H (2015) Teleconnection responses in multi-GCM driven CORDEX RCMs over Eastern Africa. *Clim Dyn*. <https://doi.org/10.1007/s00382-015-2734-7>
- Frich P, Alexander LV, Della-Marta P, Gleason B, Haylock M, Tank AMGK, Peterson T (2002) Observed coherent changes in climatic extremes during the second half of the twentieth century. *Clim Res* 19:193–212
- Gbode IE, Akinsanola AA, Ajayi VO (2015) Recent changes of some observed climate extreme events in Kano. *International Journal of Atmospheric Sciences Volume 2015*, Article ID 298046, 6 pages <https://doi.org/10.1155/2015/298046>.
- Giorgi F, Jones C and Asrar G (2009). Addressing climate information needs at the regional level: the CORDEX framework. *World Meteorology Organ Bulletin* Available online at http://wcrp.ipsl.jussieu.fr/RCD_Projects/CORDEX/CORDEX_giorgi_WMO.pdf., 58, 175–183
- Hartmann DL, Klein Tank AMG, Rusticucci M, Alexander LV, Brönnimann S, Charabi Y, Dentener FJ, Dlugokencky EJ, Easterling DR, Kaplan A, Soden BJ, Thorne PW, Wild M, Zhai PM (2013) Observations: atmosphere and surface. In: *Climate change 2013: the physical science basis*. In: Stocker TF, Qin D, Plattner G-K, Tignor M, Allen SK, Boschung J, Nauels A, Xia Y, Bex V, Midgley PM (eds) *Contribution of Working Group I to the Fifth Assessment Report of the Intergovernmental Panel on Climate Change*. Cambridge University Press, Cambridge and New York
- IPCC (2012) *Managing the risks of extreme events and disasters to advance climate change adaptation*. In: Field CB, Barros V, Stocker TF, Qin D, Dokken DJ, Ebi KL, Mastrandrea MD, Mach KJ, Plattner G-K, Allen SK, Tignor M, Midgley PM (eds) *A Special Report of Working Groups I and II of the Intergovernmental Panel on Climate Change*. Cambridge University Press, Cambridge and New York 582 pp
- IPCC (2013) *Climate change 2013. The physical science basis. Headline Statements from the Summary for Policymakers*, 2pp
- Jones C, Giorgi F, Asrar G (2011) The coordinated regional downscaling experiment: CORDEX, an international downscaling link to CMIP5. *CLIVAR Exchanges* 56(16):34–40
- Kim J, Waliser DE, Mattnann CA, Goodale CE, Hart AF, Zimdars PA, Crichton DJ, Jones C, Nikulin G, Hewitson B, Jack C, Lennard C, Favre A (2014) Evaluation of the CORDEX-Africa multi-RCM hindcast: systematic model errors. *Clim Dyn* 42:1189–1202 <https://doi.org/10.1007/s00382-013-1751-7>
- Klein Tank AMG, Zwiers FW, Zhang X (2009) Guidelines on analysis of extremes in a changing climate in support of informed decisions for adaptation, *Climate data and monitoring WCDMP-No. 72*, WMO-TD No. 1500, 56pp
- Klutse NAB, Sylla MB, Diallo I, Sarr A, Dosio A, Diedhiou A, Kamga A, Lamptey B, Ali A, Gbobaniyi EO, Owusu K, Lennard C, Hewitson B, Nikulin G, Panitz H-J, Bucher M (2014) Daily characteristics of West African summer monsoon precipitation in CORDEX simulations. *Theoretical and Applied Climatology*. <https://doi.org/10.1007/s00704-014-1352-3>
- Kruger AC, Sekele SS (2013) Trends in extreme temperature indices in South Africa: 1962–2009. *Int J Climatol* 33:661–676. <https://doi.org/10.1002/joc.3455>
- Maraun D (2016) Bias correcting climate change simulations - a critical review. *Curr Clim Change Reports*. <https://doi.org/10.1007/s40641-016-0050-x>
- Maraun D, Wetterhall F, Ireson AM, Chandler RE, Kendon EJ, Widmann M, Brienen S, Rust HW, Sauter T, Themeßl M, Venema VKC, Chun KP, Goodess CM, Jones RG, Onof C, Vrac M, Thiele-Eich I (2010) Precipitation downscaling under climate change: recent developments to bridge the gap between dynamical models and the end user. *Rev Geophys* 48:RG3003
- Marinucci MR, Giorgi F (1992) A 2XCO2 climate change scenario over Europe generated using a limited area model nested in a general circulation model 1. Present-day seasonal climate simulation. *J Geophys Res* 97(D9):9989–10,009. <https://doi.org/10.1029/92JD00615>
- Mekasha A, Tesfaye K, Duncan AJ (2014) Trends in daily observed temperature and precipitation extremes over three Ethiopian environments. *Int J Climatol* 34:1990–1999
- Moss RH, Edmonds JA, Hibbard KA, Manning MR, Rose SK, van Vuuren DP, Carter TR, Emori S, Kainuma M, Kram T, Meehl GA, Mitchell JF, Nakicenovic N, Riahi K, Smith SJ, Stouffer RJ, Thomson AM, Weyant JP, Wilbanks TJ (2010) The next generation of scenarios for climate change research and assessment. *Nature* 463:747–756
- Mouhamed L, Traore SB, Alhassane A, Sarr B (2013) Evolution of some observed climate extremes in the West African Sahel. *Weather and Climate Extremes* 1:19–25
- Murphy J (1999) An evaluation of statistical and dynamical techniques for downscaling local climate. *J Clim* 12(8):2256–2284
- New M, Hewitson B, Stephenson DB, Tsiga A, Kruger A, Manhique A, Gomez B, Coelho CAS, Masisi DN, Kululanga E, Mbambalala E, Adesina F, Saleh H, Kanyanga J, Adosi J, Bulane L, Fortunata L, Mdoka ML, Lajoie R (2006) Evidence of trends in daily climate extremes over southern and west Africa Evidence of trends in daily climate extremes over southern and West Africa. *J Geophys Res* 111:D14102
- Nikulin G, Jones C, Giorgi F, Asrar G, Büchner M, Cerezo-Mota R, Christensen OB, Déqué M, Fernandez J, Hänsler A et al (2012) Precipitation climatology in an ensemble of CORDEX-Africa regional climate simulations. *J Clim* 25(18):6057–6078. <https://doi.org/10.1175/JCLI-D-11-00375.1>
- Orlowsky B, Seneviratne SI (2011) Global changes in extreme events: regional and seasonal dimension. *Clim Chang* 110:669. <https://doi.org/10.1007/s10584-011-0122-9>
- Oyebande L, Odunuga S (2010) Climate change impact on water resources at the transboundary level in West Africa: the cases of the Senegal, Niger and Volta Basins. *Open Hydrol J* 4:163–172
- Paeth H, Hall NMJ, Gaertner MA, Alonso MD, Moumouni S, Polcher J, Ruti PM, Fink AH, Gosset M, Lebel T, Gaye AT, Rowell DP, Moufouma-Okia W, Jacob D, Rockel B, Giorgi F, Rummukainen M (2011) Progress in regional downscaling of West African precipitation. *Atmospheric science letters* doi:asl.306., 12, 75–82

- Panitz HJ, Dosio A, Büchner M, Lüthi D, Keuler K (2014) COSMO-CLM (CCLM) climate simulations over CORDEXAfrica domain: analysis of the ERA-interim driven simulations at 0.44 and 0.22 resolution. *Clim Dyn*. <https://doi.org/10.1007/s00382-013-1834-5>
- Peel MC, Finlayson BL, McMahon TA (2007) Updated world map of the Köppen-Geiger climate classification. *Hydrol Earth Syst Sci* 11: 1633–1644. <https://doi.org/10.5194/hess-11-1633-2007>
- Pinto I, Lennard C, Tadross M, Hewitson B, Dosio A, Nikulin G, Panitz H-J, Shongwe M (2016) Climatic Change 135(3–4):655–668. <https://doi.org/10.1007/s10584-015-1573-1>
- Sarr B (2011) Return of heavy downpours and floods in a context of changing climate. *Climate change in the Sahel. A challenge for sustainable development*. AGRHYMET Monthly Bulletin, 9-11. <http://www.agrhymet.ne/PDF/Bulletin%20mensuel/specialChCang.pdf>. 2 October 2015.
- Sarr MA, Seidou O, Trambly Y, Adlouni S El (2015). Comparison of downscaling methods for mean and extreme precipitation in Senegal. *J Hydrol Reg Stud*, 4, 369–385
- Sillmann J, Kharin VV, Zwiers FW, Zhang X, Bronaugh D (2013) Climate extremes indices in the CMIP5 multimodel ensemble: part 2. Future climate projections. *J Geophys Res Atmos* 118:2473–2493. <https://doi.org/10.1002/jgrd.50188>
- Solomon S, Qin D, Manning M, Chen Z, Marquis M, Averyt K, Tignor M, Miller H.L (2007). Contribution of Working Group I to the Fourth Assessment Report of the Intergovernmental Panel on Climate Change. *Climate Change 2007: The Physical Science Basis*. Cambridge University Press, Cambridge
- Sylla MB, Nikiema PM, Gibba P, Kebe I, Klutse NAB (2016) Climate change over West Africa: recent trends and future projections climate change over West Africa: recent trends and future projections. <https://doi.org/10.1007/978-3-319-31499-0>
- Ta S, Kouadio KY, Ali KE, Toualy E, Aman A, Yoroba F (2016) West Africa extreme rainfall events and large-scale ocean surface and atmospheric conditions in the tropical Atlantic. *Advances in meteorology*, Hindawi Publishing Corporation, Article ID 1940456, 14 pp. <https://doi.org/10.1155/2016/1940456>
- Taylor KE, Stouffer RJ, Meehl GA (2012) An overview of CMIP5 and the experiment design. *Bull Am Meteorol Soc* 93(4):485–498. <https://doi.org/10.1175/BAMS-D-11-00094.1>
- Themeßl MJ, Gobiet A, Leuprecht A (2011a) Empirical-statistical downscaling and error correction of daily precipitation from regional climate models – Jakob Themeßl, Wiley Online Library. *Int J Climatol* 31:1530–1544
- Themeßl MJ, Leuprecht A (2011b) Empirical-statistical downscaling and error correction of daily precipitation from regional climate models. *Int J Climatol* 31:1531–1544
- Tschakert P, Sagoe R, Ofori-Darko G, Codjoe SN (2010) Floods in the Sahel: an analysis of anomalies, memory, and anticipatory learning. *Climate Change* 103(3–4):471–502. <https://doi.org/10.1007/s10584-009-9776-y>
- Xu Z, Yang Z-L (2015) A new dynamical downscaling approach with GCM bias corrections and spectral nudging. *J Geophys Res Atmos*. <https://doi.org/10.1002/2014JD022958>
- Zhang X, Yang F (2004) RCLimdex (1.0) user manual. <http://cccma.seos.uvic.ca/ETCCDMI/software.shtml>. 4 Jan 2015.
- Zhang X, Alexander L, Hegerl GC, Jones P, Klein Tank A, Peterson TC, Trewin B, Zwiers FW (2011) Indices for monitoring changes in extremes based on daily temperature and precipitation data. *WIREs Clim Change* 2:851–870

Terms and Conditions

Springer Nature journal content, brought to you courtesy of Springer Nature Customer Service Center GmbH (“Springer Nature”).

Springer Nature supports a reasonable amount of sharing of research papers by authors, subscribers and authorised users (“Users”), for small-scale personal, non-commercial use provided that all copyright, trade and service marks and other proprietary notices are maintained. By accessing, sharing, receiving or otherwise using the Springer Nature journal content you agree to these terms of use (“Terms”). For these purposes, Springer Nature considers academic use (by researchers and students) to be non-commercial.

These Terms are supplementary and will apply in addition to any applicable website terms and conditions, a relevant site licence or a personal subscription. These Terms will prevail over any conflict or ambiguity with regards to the relevant terms, a site licence or a personal subscription (to the extent of the conflict or ambiguity only). For Creative Commons-licensed articles, the terms of the Creative Commons license used will apply.

We collect and use personal data to provide access to the Springer Nature journal content. We may also use these personal data internally within ResearchGate and Springer Nature and as agreed share it, in an anonymised way, for purposes of tracking, analysis and reporting. We will not otherwise disclose your personal data outside the ResearchGate or the Springer Nature group of companies unless we have your permission as detailed in the Privacy Policy.

While Users may use the Springer Nature journal content for small scale, personal non-commercial use, it is important to note that Users may not:

1. use such content for the purpose of providing other users with access on a regular or large scale basis or as a means to circumvent access control;
2. use such content where to do so would be considered a criminal or statutory offence in any jurisdiction, or gives rise to civil liability, or is otherwise unlawful;
3. falsely or misleadingly imply or suggest endorsement, approval, sponsorship, or association unless explicitly agreed to by Springer Nature in writing;
4. use bots or other automated methods to access the content or redirect messages
5. override any security feature or exclusionary protocol; or
6. share the content in order to create substitute for Springer Nature products or services or a systematic database of Springer Nature journal content.

In line with the restriction against commercial use, Springer Nature does not permit the creation of a product or service that creates revenue, royalties, rent or income from our content or its inclusion as part of a paid for service or for other commercial gain. Springer Nature journal content cannot be used for inter-library loans and librarians may not upload Springer Nature journal content on a large scale into their, or any other, institutional repository.

These terms of use are reviewed regularly and may be amended at any time. Springer Nature is not obligated to publish any information or content on this website and may remove it or features or functionality at our sole discretion, at any time with or without notice. Springer Nature may revoke this licence to you at any time and remove access to any copies of the Springer Nature journal content which have been saved.

To the fullest extent permitted by law, Springer Nature makes no warranties, representations or guarantees to Users, either express or implied with respect to the Springer nature journal content and all parties disclaim and waive any implied warranties or warranties imposed by law, including merchantability or fitness for any particular purpose.

Please note that these rights do not automatically extend to content, data or other material published by Springer Nature that may be licensed from third parties.

If you would like to use or distribute our Springer Nature journal content to a wider audience or on a regular basis or in any other manner not expressly permitted by these Terms, please contact Springer Nature at

onlineservice@springernature.com